The Nucleocapsid Protein of SARS-CoV Induces Transcription of hfgl2 Prothrombinase Gene Dependent on C/EBP Alpha

Meifang Han[1,2], Weiming Yan[1,2], Yuancheng Huang[1,2], Huaning Yao[1,2], Zhanhui Wang[3], Dong Xi[1,2], Weina Li[1,2], Yaoyong Zhou[1,2], Jinlin Hou[3], Xiaoping Luo[2,4] and Qin Ning[1,2],*

[1]*Department of Infectious Disease;* [2]*Tongji Hospital of Tongji Medical College, Huazhong University of Science and Technology, Wuhan, 430030;* [3]*Department of Infectious Disease, Nanfang Hospital, Southern Medical University, Guangzhou, 510515; and* [4]*Department of Pediatrics, Huazhong University of Science and Technology, Wuhan, 430030, China*

Fibrin deposition was universal in the lungs of SARS patients and fgl2 prothrombinase gene, a novel procoagulant, was demonstrated to express highly in a clinically relevant SARS model. To investigate whether and which structural protein of SARS-CoV induced transcription of hfgl2 prothrombinase gene, three eukaryotic expression plasmids expressing nucleocapsid protein (N), membrane protein (M) and spike protein 2 (S2) of SARS-CoV were co-transfected with hfgl2 promoter luciferase-reporter plasmids and β-galactosidase plasmid in CHO cells, respectively. M, N and S2 protein of SARS-CoV were detected by western blotting and immunohistochemistry analysis. Further assays demonstrated that expression of hfgl2 gene was related with N protein, but not with M or S2 protein in THP-1 cells and Vero cells. N protein significantly induced functional procoagulant activity in comparison with control group. Luciferase assay showed that N protein of SARS-CoV could activate the transcription of hfgl2 promoter compared with the pcDNA3.1 empty vector. Site-directed mutagenesis and EMSA assay further demonstrated that transcription factor C/EBP alpha band with its cognate cis-element in hfgl2 promoter. The results showed that N protein of SARS-CoV induced hfgl2 gene transcription dependent on the transcription factor C/EBP alpha, which maybe contribute to the development of thrombosis in SARS.

Key words: gene regulation, hfgl2, nucleocapsid protein, prothrombinase, SARS-CoV.

Abbreviations: fgl2, fibrinogen-like protein-2; hfgl2, human fibrinogen-like protein-2; mfgl2, mouse fibrinogen-like protein-2; SARS, severe acute respiratory syndrome; SARS-CoV, severe acute respiratory syndrome associated coronary virus.

Activation of the coagulant system represents an important facet of immune and inflammatory reactions, accounting for the fibrin deposition that is commonly observed in these reactions. Cellular procoagulants and the soluble factors of the coagulation cascade are important participants in a number of human diseases including allograft rejection (*1*), glomerulonephritis (*2*), septic shock (*3*) and bacterial and rival infections (*4*). Fgl2 (fibrinogen-like protein-2) prothrombinase also named fgl2 fibroleukin, was determined to encode an immune coagulant and was localized to the proximal region of mouse chromosome 5 (*5*, *6*). Both hfgl2 (human fgl2) and mfgl2 (mouse fgl2) gene encode a serine protease capable of directly cleaving prothrombin to thrombin, resulting in intra-vascular fibrin deposition within the liver and culminating in widespread hepatocyte necrosis (*7–11*). As procoagulants, fgl2 plays an important role in the development of murine hepatitis virus type 3 (MHV-3) induced fulminant hepatitis and human severe acute chronic hepatitis B (*12*). Fgl2 gene

was also demonstrated to be involved in pathogenesis of experimental and human allograft rejection and spontaneous abortion (*13*).

As a new serious and fatal infectious disease, severe acute respiratory syndrome (SARS) outbreak spread over Asia to Europe and North America in November 2002. SARS associated coronavirus (SARS-CoV) is demonstrated to be the aetiological agent of SARS. Morphological changes from SARS patients are summarized as diffuse and bilateral lung consolidation and diffuse alveolar damage with hyaline membrane formation (*14*, *15*). Apart from intra-alveolar oedema/haemorrhage and pneumocyte desquamation, fibrin deposition was universal. Recently, it has been noted that hfgl2 prothrombinase gene may be involved in the immune coagulation in SARS (*16*). In a clinically relevant model of SARS, fgl2 mRNA transcripts and protein and fibrin deposits were markedly increased in the lungs of A/J mice infected with murine hepatitis virus 1 (*17*). These observations supported that high expression of fgl2 may be involved in the development of SARS.

Molecular biological analyses of SARS-CoV identified 13–15 open reading frames (ORFs) (*18*). Apart from

replicase and protease, the SARS-CoV genome encodes several structural proteins: spike (S), envelope (E), membrane protein (M), nucleocapsid protein (N) (*19*, *20*). Among these well-known genes, a series of ORFs with unknown function were found. SARS-CoV 7a protein was demonstrated to inhibit Cellular Protein Synthesis and activate p38 Mitogen-Activated Protein Kinase (*21*). Non-structural protein 10 of SARS-CoV had the interaction with the cellular oxido-reductase system and caused an extensive cytopathic effect. Non-structural protein 1 of SARS-CoV played an important role in CCL5, CXCL10 and CCL3 expression in human lung epithelial cells via the activation of NF-kappaB (*22*). Furthermore, researchers investigated the possible regulatory interaction between the SARS-CoV nucleocapsid (N) protein and NF-κB and showed that N protein of SARS-CoV can significantly activate NF-κB only in Vero E6 cells (*23*). In addition, SARS-CoV N protein was demonstrated to activate the expression of cyclooxygenase-2 by binding directly to regulatory elements for nuclear factor-kappa B and CCAAT/enhancer binding protein (*24*). These viral structural and non-structural proteins were shown to be involved in the regulation of host genes. In this study, we constructed three SARS-CoV protein eukaryotic expression plasmids and investigated the roles of SARS-CoV proteins in regulation of hfgl2 prothrombinase gene. Our study demonstrated that nucleocapsid protein of SARS-CoV activated hfgl2 prothrombinase dependent on the transcription factor C/EBP alpha and contributed to the fibrin deposition in SARS.

MATERIALS AND METHODS

Construction of Eukaryotic Expression Plasmids pcDNA-S2, pcDNA-M and pcDNA-N—Total RNA was extracted from the lung tissues of SARS patients which were confirmed by the diagnostic criteria of Chinese Ministry of Public Health announced on Apri1 5, 2003, which was consistent with the diagnostic criteria of Centers for Disease Control and Prevention (CDC) (http://www.cdc.gov/ncidod/sars/casedefinition.htm). RT-PCR was performed according to the manuscript of reversed transcriptive enzyme. S2, M and N gene were amplified by PCR using the cDNA as template. S2 and N gene of SARS were cloned into the prokaryotic expression vector pET28, while M gene was cloned into the vector pET32. Three pairs of primers N1/N2, M1/M2, S1/S2 (N1, 5′-CTC GGA TCC ATG TCT GAT AAT GGA CCC C-3′, N2, 5′-CTG GCG GCC GCT GCC TGA GTT GAA TCA GCA G-3′, M1, 5′- CTC GGA TCC ATG GCA GAC AAC GGT AC-3′, M2, 5′-CTG CTC GAG TTA CTG TAC TAG CAA AGC-3′, S1, 5′-CTC GGA TCC CAT GTC GAC ACT TCT TAT G-3′, and S2, 5′-CCT GCT CGA GTA TAT TGC TCA T-3′) were used to amplify N, M and S2 genes with the products of 1,266, 666 and 1,653 bp, respectively. The sequence of SARS-CoV was novel and submitted to Genebank (AY390556) (*25*). The expression of SARS-CoV S2, M and N protein was detected in prokaryotic expression system. SARS-CoV S2 and M gene fragment was released from pET28-S2 and pET32-M by digestion with BamH I and Xho I and then subcloned into

eukaryotic expression vector pcDNA3.1 (+) using the BamH I and Xho I sites to form pcDNA-S2 and pcDNA-M. SARS-CoV N gene fragment was released from pET28-N by digestion with BamH I and Not I and then subcloned into pcDNA3.1 (+) using the BamH I and Not I sites to form eukaryotic expression plasmid pcDNA-N.

Construction of hfgl2 Promoter Luciferase-Reporter Plasmids—Fgl2 promoter luciferase-reporter plasmids were constructed as described previously (*9*). Briefly, a 1.3-kb DNA fragment including the entire hfgl2 gene promoter was released by restriction digestion with EcoRV and SalI from a subclone pBluescript-m166 (pm166) of human genomic P1 plasmid (Genome System Inc., USA) that contains the entire hfgl2 gene. The isolated 1.3-kb fragment was then inserted into SmaI and XhoI sites of the pGL2-Basic luciferase-reporter vector (pGL2-Basic, Promega, USA) to form hfgl2 promoter luciferase-reporter plasmid hfgl2p(-1334)LUC. 5′-truncation of the hfgl2 promoter in pGL2-Basic was carried out by PCR using hfgl2p(-1334)LUC as template. The series PCR products were respectively cloned into PCR2.1 cloning vector and subcloned into pGL2-Basic plasmid at HindIII and XhoI sites to form four 5′ truncation of hfgl2 promoter luciferase-reporter constructs. The upstream primers used were 5′-CTT ATG TCT TTC CTG CCT TC-3′ for hfgl2p(-998)LUC, 5′-GGC AAG AGA AGT TCA GGA C-3′ for hfgl2p(-817)LUC, 5′-AAT ACA GGC TCC CCA ATG C-3′ for hfgl2p (-467)LUC and 5′-GTG AAT CTT GTT GGC TGT G-3′ for hfgl2p(-243)LUC. The common downstream primer used was 5′-TTC GCC CAT CTT TAC AGTG-3′. The promoter luciferase-reporter plasmids were all sequenced to confirm the orientation and to verify the sequence.

Cell Culture and Transient Transfections—CHO cell line was cultured with F12 medium (Gibco, USA), and human macrophage cell line THP-1 cell line was cultured with 1,640 medium, and both media were supplemented with 10% FBS. African green monkey kidney (Vero) cells were cultured in DMEM with 5% FCS. Cells were plated in six-well culture plates at 50–70% confluency. Two micrograms of expression plasmid pcDNA-N, pcDNA-M or pcDNA-S2, 1 μg hfgl2p(-1334)LUC plasmid, 0.5 μg β-galactosidase plsmid (as a marker for transfection efficiency by β-galactosidase assay, Rous sarcoma virus β-galactosidase vector were purchased from Promega company) in 100 μl Opti-MEM medium (Invitrogen, USA) were mixed by vortexing with 8 μl of Lipofectamine 2000 (Invitrogen, USA) in 100 μl Opti-MEM medium. After incubation of the mixture at room temperature for 20 min, 1.8 ml Opti-MEM medium (Invitrogen, USA) was added to bring up the volume to 2 ml. One millilitre of the mixture was distributed into one of the duplicated wells with cells. After cells were cultured for 10–12 h, another 1 ml culture medium was added to the well. Transfection was performed at 37°C with 5% CO_2 for 40–44 h. After transfection, these cells were harvested to measure expression of SARS-CoV M, N and S2 proteins by immunocytochemistry.

Western Blotting to Detect SARS-CoV Protein—CHO Cells transcfected with pcDNA-N, pcDNA-M or pcDNA-S2 were lysed respectively in a lysis buffer containing

150 mM NaCl, 50 mM Tris, pH 7.4, 5 mM EDTA, 1% NP-40 and protease inhibitors for 30 min on ice, and whole-cell lysate was obtained by subsequent centrifugation. Samples were heated at 100°C for 5 min and cooled on ice. Fifty micrograms of protein from whole-cell lysates was subjected to 12% SDS–PAGE and transferred to a nitrocellulose membrane (Bio-Rad). Biotinylated protein ladder detection pack 7727 (Cell Signaling, USA) was used as protein ladder. Blocking was performed in 5% (w/v) non-fat dried milk in phosphate-buffered saline (PBS) containing 0.1% Tween-20 and then incubated with the anti-SARS-CoV-S2, anti-SARS-CoV-M and anti-SARS-CoV-N polyclonal antibodies from rabbit (provided by Prof. Hu Zhi-hong, Key Laboratory of Molecular Virology, Wuhan Institute of Virology, Chinese Academy of Sciences wuhan virus research, China) with 1:400 dilution overnight followed by a secondary horseradish peroxidase (HRP)-labelled anti-rabbit IgG with 1:1000 dilution. At the stage of secondary antibody incubation, anti-biotin HRP-linked antibody was added according to the protein ladder's instruction. The peroxidase-based detection was performed with Super Signal West Pico Chemiluminescent Subatrates Kits (Pierce, USA) according to the manufacturer's instructions.

Immunocytochemistry to Detect SARS-CoV Protein— CHO Cells transfected with pcDNA-S2, pcDNA-M or pcDNA-N were fixed with 80% acetone for 10 min and then incubated in the 3% H_2O_2 to block internal peroxidase for 10 min at room temperature. Then cells were incubated for 10 min at room temperature in blocking solution of normal goat serum according to the manufacturer's instructions (SP kits, Sigma, USA). The cells were stained with the anti-SARS-CoV-S2, anti-SARS-CoV-M or anti-SARS-CoV-N polyclonal antibodies from rabbit with 1:200 dilution overnight followed by a secondary biotinylated anti-rabbit IgG with 1:1000 dilution. Solution of streptavidin-peroxidase was added to cells. As negative controls, CHO cells, either without transfection or transfected with pcDNA3.1(+) empty vector was employed.

Real-Time Fluorescence Quantitative RT-PCR— Previous research found that hfgl2 expression is confined in macrophage cells, lymphocytes and endothelial cells of intrahepatic veins and hepatic sinusoids. THP-1 cell line was a monocyte cell line. Vero cell was demonstrated to be one of susceptible cells line to SARS CoV. Therefore, THP-1 and Vero cell lines system were introduced to characterize hfgl2 gene transcript and protein expression in response to SARS-CoV proteins. Total RNA was extracted from THP-1 cells and Vero cells transfected with pcDNA-S2, pcDNA-M or pcDNA-N with TRIzol reagent (Invitrogen, USA) according to the manufacturer's standard protocol. Total RNA extracted from cells transfected was identified with ribonuclease-free gel and spectrophotometer. The cDNA of every transfection group was produced with reversed transcriptive enzyme (Promega, USA). Real-time fluorescence quantitative RT-PCR was done with EvaGreen PCR reagents (Biotium, USA) according to the manufacturer's standard protocol to detect mRNA level of hfgl2. The upstream primer was 5′-ACT GTG ACA TGG AGA CCA TG-3′, and the

downstream primer was 5′-TCC TTA CTC TTG GTC AGA AG-3′.

Western Blotting Analysis to Detect hfgl2 Prothrombinase—Cell lysates from THP-1 and Vero cells transfected with pcDNA-S2, pcDNA-M or pcDNA-N in a six-well plate were prepared by adding 0.2 ml of ice-cold buffer (20 mM Tris (pH 7.5), 150 mM NaCl, 1 mM EDTA, 1 mM EGTA, 1% Triton X-100, 2.5 mM sodium pyrophosphate) supplemented with the protease inhibitors leupeptin (1 μg/ml), anti-paptin (50 μg/ml) and PMSF (0.1 mM). Lysates were sheared by ultrasonic wave for 3 min. The lysates were centrifuged for 10 min at 4°C and the supernatants were collected. Samples were heated at 100°C for 5 min, cooled on ice and resolved by SDS–PAGE, transferred to nitrocellulose membrane and subject to antibody detection. The nitrocellulose membrane was detected in the expression of hfgl2 protein using polyclonal antibody from rabbit against hfgl2 prothrombinase (1:500 dilution). After five times washing, the membranes were probed with a horseradish peroxidase-labelled goat anti-rabbit secondary antibody (Santa Cruz Biotechnology, USA) for 1 h. The peroxidase-based detection was performed with Super Signal West Pico Chemiluminescent Subatrates Kits (Pierce, USA) according to the manufacturer's instructions.

PCA Assay—The THP-1 cells and Vero cells transfected with pcDNA-S2, pcDNA-M or pcDNA-N were evaluated for functional hfgl2 prothrombinase activity in a one-stage clotting assay, as previously described (*4*, *26*). Briefly, after incubation, samples were washed three times with unsupplemented RPMI 1640 and re-suspended to a final concentration of 10^6 cells/ml. After being frozen and thawed three times, samples were assayed for the ability to shorten the spontaneous clotting time of normal citrated human platelet-poor plasma. Milliunits of activity were assigned by reference to a standard curve generated with serial log dilutions of a standard of rabbit brain thromboplastin (Dade Behring, Deerfield, IL, USA).

Luciferase Assay and Mapping of the hfgl2 Promoter— Cells transfected with pcDNA-S2, pcDNA-M, pcDNA-N and luciferase-reporter vector hfgl2p(-1334) LUC were collected and lysed in $1 \times$ lysis buffer (Promega, USA). Luciferase activity and β-galactosidase activity were assayed by using the luciferase and β-galactosidase enzyme assay system (Promega, USA). Aliquots of supernatant were assayed for luciferase activity to measure promoter activation. Values were normalized with β-galactosidase levels and calculated as an average of three independent experiments. PGL2-Basic vector was used as a negative control. Furthermore, mapping of the hfgl2 promoter was done to identify the regulatory region of hfgl2 gene in response to N protein of SARS-CoV. A series of 5′ truncated hfgl2 promoter/report constructs hfgl2p(-1334)LUC, hfgl2p(-998)LUC, hfgl2p (-817)LUC, hfgl2p(-467)LUC and hfgl2p(-243)LUC was respectively co-transfected with pcDNA-N and β-galactosidase plasmid to CHO cells as previously described. After incubation for 40–44 h, cells were lysed to detect the luciferase activity and β-galactosidase enzyme activity.

Table 1. **Primer pairs used to construct hfgl2 promoter mutants.**

Mutants name	Sequence change	Sense primer sequence (5′–3′)/antisense primer sequence (5′–3′)
C/EBP-mut	ATT to GCC	GCT GTG GAA GAT GAC AGT ACA **GCC** ACC AAA ATG TCG AAG GGC/GCC CTT CGA CAT TTT GGT **GGC** TGT ACT GTC ATC TTC CAC AGC
Nkx-2mut	AATTAT to GCCGCG	CAG CTA CTG GTT TTG ATG AAA GAC **GCC GCG** GTC CTT TTA AAT GGG TCT TAG AC/GTC TAA GAC CCA TTT AAA AGG **ACC GCG GC**G TCT TTC ATC AAA ACC AGT AGC TG
LEF-1/c-Etsmut	AGGA to CACG	CAC TAT GCT ACG GAC AA**C ACG** ATA GAA AGT AGC ACT TTT TTC TCC ACT AG/CTA GTG GAG AAA AAA GTG **CTA CTT** TCT AT**C GTG** TTG TCC GTA GCA TAG TG
HSTFmut	AGA to TCG	CAC TAT GCT ACG GAC AAA GGA AT**T CGA** AGT AGC ACT TTT TTC TCC ACT AG/CTA GTG GAG AAA AAA GTG CTA CTT **CGA** ATT CCT TTG TCC GTA GCA TAG TG
SRYmut	TAG to GGC	GAA AGT AGC ACT TTT TTC TCC AC**G GC**T TTT CTT CTC TTT TTC AAG TAG ATG AAG C/GCT TCA TCT ACT TGA AAA AGA **GAA** GAA AA**G CC**G TGG AGA AAA AAG TGC TAC TTT C
Evi-1mut	CTT to GCC	GTA GCA CTT TTT TCT CCA CTA GTT TT**G CC** C TCT TTT TCA GTA GAT GAA GC/GCT TCA TCT ACT TGA AAA AGA G**GG C**AA AAC TAG TGG AGA AAA AAG TGC TAC

Mutations were made to the promoter sequence of hfgl2 gene by a site-directed mutagenesis protocol as described under ''MATERIALS AND METHODS''. Sense and antisense primers were designed to encode the desired mutations. The underlined and bold letters indicate the mutant sequences. All constructs generated were sequenced to confirm the orientation and to verify the sequence.

Site-Directed Mutagenesis and Luciferase Assays— Constructs bearing mutant promoter variants of the hfgl2 gene were generated by PCR using the wild-type hfgl2 promoter/luciferase report construct hfgl2p (-1334)LUC as template according to the manufacturer's protocol in the QuickChange™ Site-directed Mutagenesis kit (Stratagene, USA). Six site-directed mutants were created in the C/EBP (CCAAT enhancer binding protein), Nkx-2 (a tinman homoeodomain factor), LEF-1 (lymphocyte enhancer factor-1)/c-Ets-2 (v-ets erythroblastosis virus E26 oncogene homologue 2), HSTF (heat–shock transcription factor), SRY (a sex-determining region Y gene product) and Evi-1 (an ectopic viral integration site 1 encoded factor) putative *cis*-elements located within a region (–817 to –467) of the hfgl2 promoter. Primers were designed according to manufacturer's instruction and produced by Invitrogen as shown in Table 1. The bold and underlined nucleotides indicate mutated sequences. The PCR product with 1 μl Dpn I enzyme was incubated in 37°C for 1 h. Then 5 μl of the reaction was taken out to transform XL1-Blue supercompetent cells and finally mutants were verified by sequencing. Hfgl2 promoter mutants were co-transfected with pcDNA-N expression plasmid and β-galactosidase construct in THP-1 cells and Vero cells. After transfection for 44 or 48 h, cells were lysed for detection of luciferase activity and β-galactosidase enzyme activity.

Electrophoretic Mobility Shift Assay (EMSA)—Nuclear and cytoplasmic extracts from THP-1 cells and Vero cells after transfecting with pcDNA-N were prepared as described previously (9). The sense and anti-sense probes synthesized were annealed in anneal buffer (Invitrogen, USA) to form double-stranded DNA probes. The probes were then labelled with 50 μCi [γ-32P] ATP (Beijing Furui, China) using T4 polynucleotide kinase (Takara, Japan) at 37°C for 1 h. For each EMSA reaction, 5 μg of nuclear extracts from THP-1 cells or Vero cells after transfection were incubated for 30 min at room temperature in 20 μl binding buffer (10 mM Tris–HCl, pH 7.5, 50 mM NaCl, 0.5 mM DTT, 10% glycerol, 0.05% NP-40, 5 μg of poly(dI–dC), 50 mM NaCl and 5 mM MgCl₂). A total of 10^4 dpm of probes was added to each reaction and the mixture was incubated at room temperature for 30 min. For super shift reactions, the nuclear extracts were incubated with 1 μg of specific antibody of anti-C/EBP alpha (Santa Cruz) for 30 min at room temperature before adding DNA probe. The binding reactions were size-fractionated on a non-denaturing 8% non-denaturing polyacrylamide gel, and run at 150 V at room temperature for 2 h in Tris–glycine buffer. Sequence for probes named C/EBP-hfgl2 was 5′-CTG TGG AAG ATG ACA GTA CAA TTA CCA AAA TGT CGA AGG GCA AAG GAG GCA G-3′.

Statistical Analysis—Data were expressed as means ± SD where applicable. Student's *t*-test for unpaired samples (two-tailed) was used to analyse the data using the SPSS 12 statistical software.

RESULTS

Identification of pcDNA-S2, pcDNA-M and pcDNA-N— Electrophoretic identification of recombinant plasmids pcDNA-S2, pcDNA-M and pcDNA-N by restriction enzyme were observed (data not shown). Agarose gel electrophoresis showed that pcDNA-M and pcDNA-S2 could be digested by BamHI and XhoI restriction enzyme with a 666-bp and a 1,653-bp fragment after 3 h digestion, respectively. The construction of pcDNA-N could be digested by BamHI and NotI restriction enzyme with a 1,266-bp fragment after digestion. The orientation and gene sequences of these three plasmids were confirmed by DNA sequencing.

Identification of hfgl2 Promoter Luciferase-Reporter Plasmids—Electrophoretic identification of recombinant plasmids hfgl2p(-998)LUC, hfgl2p(-817)LUC, hfgl2p (-467)LUC and hfglp2(-243)LUC by restriction enzyme were observed (data not shown). Agarose gel electrophoresis showed that hfgl2p(-998)LUC, hfgl2p(-817)LUC, hfgl2p(-467)LUC and hfglp2(-243)LUC could be digested by HindIII and XhoI restriction enzyme respectively with about 1,008, 827, 477 and 253-bp fragment after digestion. All above sequences were confirmed by DNA sequencing.

Expression of SARS-CoV N, M and S2 Proteins in CHO Cells—To determine the expression of SARS-CoV N,
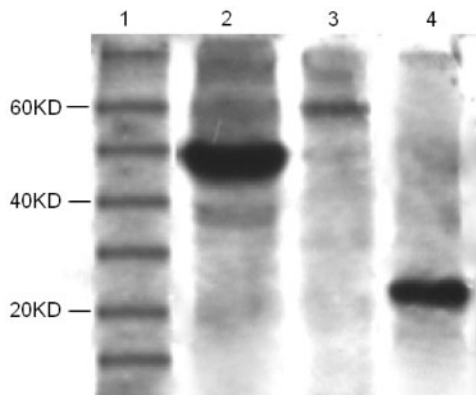
Fig. 1. **Western blotting assay to detect the expression of SARS-CoV S2, M and N proteins.** CHO cells were transfected with pcDNA-M, pcDNA-N, pcDNA-S2, respectively for 40–44 h, and were harvested to detect the expression of SARS-CoV proteins. Three expected bands were specifically seen with the size of 47, 25 and 61 kDa, respectively, consistent with the known size of the SARS-CoV N, M and S2 protein. Lane 1, protein ladder; lanes 2, 3 and 4 show the cells transfected with pcDNA-N, pcDNA-S2 and pcDNA-M, respectively.

M and S2 proteins and identify whether these eukaryotic expression plasmids were successfully constructed, western blotting and immunocytochemistry analysis were used to detect the expression of individual proteins. As shown in Fig. 1, three expected bands were specifically visualized by western blotting with the size of 47, 25 and 61 kDa, respectively consistent with the known size of the SARS-CoV N, M and S2 protein. In Fig. 2, the dark cytoplasmic staining was seen in either pcDNA-N, pcDNA-M or pcDNA-S2 transfected cells in immunocytochemistry assay, whereas there was no or trace amount of staining in pcDNA3.1 empty vector transfected cells (negative control). These results suggested the successful expression of N, M or S2 protein of SARS-CoV in CHO cells, respectively. According to our assay, the expressing of SARS-CoV structural proteins began at 24 h post-transfection, peaked at 40–44 h and followed descent. Although some reports supported N protein was detected in nuclei of cells, it was not significant in our study (*24*).

SARS-CoV N Protein Enhanced Expression of hfgl2 Prothrombinase—To evaluate the effects of SARS-CoV structural proteins on hfgl2 expression *in vitro*, a time-course study of the effects was performed by real-time fluorescence quantitative RT-PCR to detect mRNA level of hfgl2 in THP-1 cells and Vero cells (Fig. 3). The standard curve was established by using multiple-proportion-diluted plasmids containing the entire hfgl2 gene. In THP-1 cells the value of relative mRNA expression of hfgl2 induced by N protein of SARS-CoV was 6.4, whereas it was 2.4 and 2.5 induced by M and S2 protein of SARS-CoV. In Vero cells, the value of relative mRNA expression of hfgl2 induced by N protein was 5.4, whereas it was both 2.1 induced by M and S2 protein of SARS-CoV. It was evident that SARS-CoV N protein significantly enhanced hfgl2 mRNA expression compared with untreated group, whereas M and S2 protein of SARS-CoV did not. To determine the expression of hfgl2

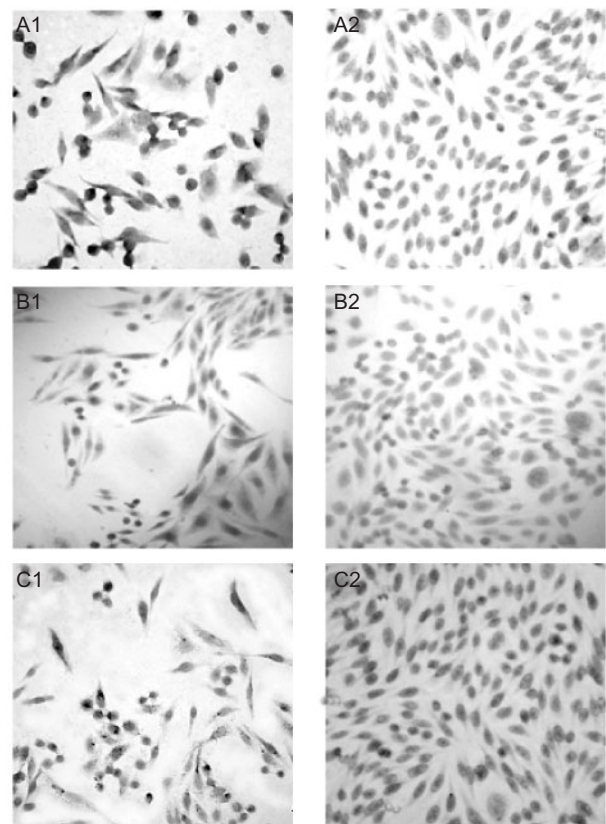Fig. 2. **Immunocytochemistry assay analysis of expression of SARS-CoV S2, M and N proteins.** CHO cells were transfected with pcDNA-M, pcDNA-N, pcDNA-S2, respectively for 40–44 h, and were harvested to detect the expression of SARS-CoV proteins. A1: indicates the marked expression of N protein of SARS-CoV in CHO cells transfected with pcDNA-N plasmid compared with control cells (A2). B1 indicates the marked expression of M protein of SARS-CoV in CHO cells transfected with pcDNA-M plasmid compared with control cells (B2). C1 indicates the marked expression of S2 protein of SARS-CoV in CHO cells transfected with pcDNA-S2 plasmid compared with control cells (C2).

on the protein level in response to SARS-CoV proteins, western blotting analysis of hfgl2 was performed in THP-1 cells and Vero cells. It was shown that hfgl2 protein was enhanced distinctly by the stimulation of SARS-CoV N protein in THP-1 cells. No hfgl2 protein was detected in the cells transfected with pcDNA-M or pcDNA-S2 (Fig. 4). The similar results were evidenced when transfection of SARS-CoV protein expression plasmid was performed in Vero cells (data not shown).

Functional Procoagulant Activity was Induced by SARS-CoV N Protein in Transfected THP-1 Cells and Vero Cells—To determine the functional activity of hfgl2 prothrombinase in response to SARS-CoV N protein, the procoagulant activity (PCA) was measured in a one-stage clotting assay. THP-1 cells and Vero cells were collected 40–44 h post-transfection with SARS-CoV proteins eukaryotic expression plasmids and PCA were measured. The mean PCA of three separate experiments induced by SARS-CoV N protein was 1,484 and 966 mU/ml in THP-1 and Vero cells, respectively, whereas it was
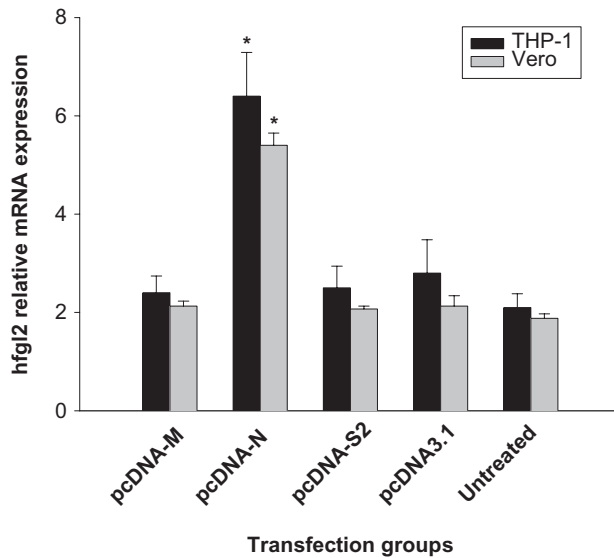
Fig. 3. Real-time PCR analysis of expression of hfgl2 in response to SARS-CoV N, M and S2 proteins. THP-1 cells and Vero cells were transfected with pcDNA-N, pcDNA-M, pcDNA-S2 and pcDNA-3.1 empty vector respectively, and untranfected cells as control group. Values represent the means $\pm$ SD of three separate experiments done in replicate. Asterisk represents a $P < 0.01$ compared with empty pCDNA transfected or untransfected THP-1 cells.
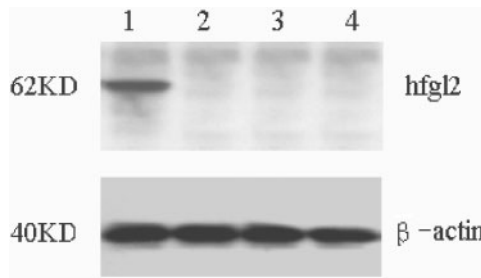

Fig. 4. Western blotting analysis of hfgl2 expression in response to SARS-CoV N, M and S2 proteins. THP-1 cells were transfected with pcDNA-N, pcDNA-M, pcDNA-S2 and pcDNA-3.1 empty vector, respectively. Lane 1: pcDNA-N; lane 2: pcDNA-M; lane 3: pcDNA-S2; lane 4: pcDNA-3.1 empty vector.

188 and 184 mU/ml in untreated group of the two cell lines. The results revealed SARS-CoV N protein significantly increased PCA in comparison with untreated group. However, the M and S2 protein of SARS-CoV did not induce increased functional PCA (Fig. 5). These data strongly demonstrated that the N protein of SARS-CoV is involved in the enhanced transcription of hfgl2 prothrombinase.

Mechanism of hfgl2 Transcription Induced by SARS-CoV N Protein—To explore the mechanism of increased expression of hfgl2 in response to SARS-CoV proteins, CHO cells were co-transfected with the hfgl2 promoter construct hfgl2p(-1334)LUC and pcDNA-N, pcDNA-M or pcDNA-S2 vectors. As shown in Fig. 6, in consistence with above real-time PCR and western blotting results, SARS-CoV N protein induced hfgl2 promoter activity
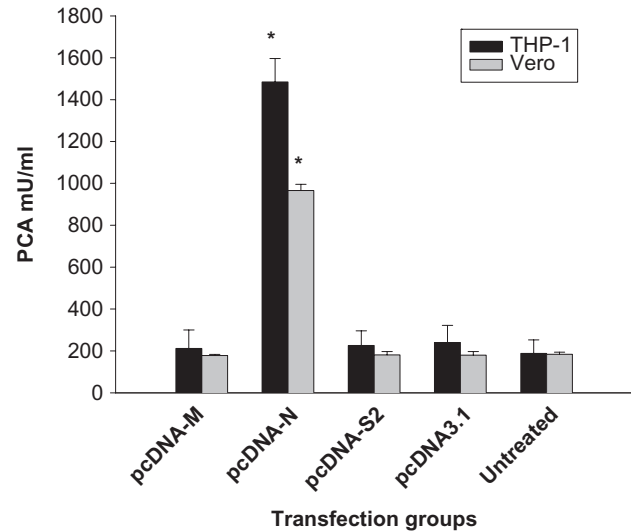

Fig. 5. Functional procoagulant activity induced by SARS-CoV proteins in transfected THP-1 cells and Vero cells. THP-1 cells and Vero cells were transfected with pcDNA-M, pcDNA-N, pcDNA-S2 and pcDNA-3.1 empty vector respectively for 40–44 h, and were harvested for measurement of procoagulant activity. Values represent the mean $\pm$ SD of three separate experiments done in replicate. Asterisk represents a $P < 0.01$ compared with pcDNA-3.1 empty vector transfected or untransfected THP-1 cells and Vero cells.
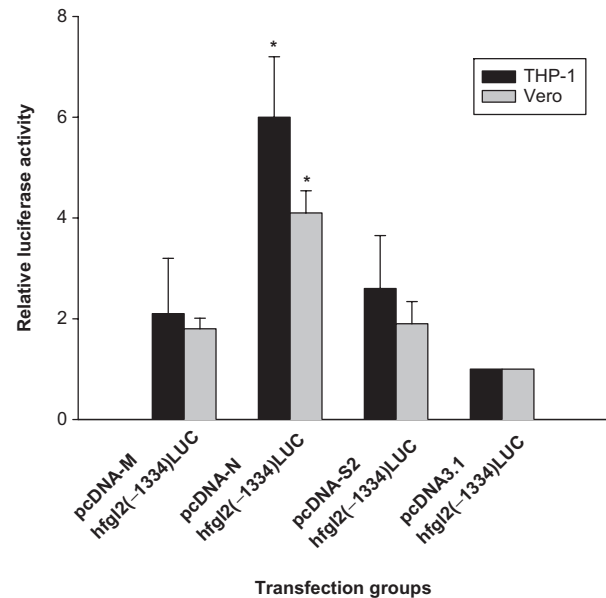

Fig. 6. SARS-CoV N protein induced transcription of hfgl2 gene. pcDNA-M, pcDNA-N or pcDNA-S2 were co-transfected with hfgl2p(-1334)LUC in THP-1 cells and Vero cells for 40–44 h, and cells were harvested for measurement of luciferase activity. Values represent the means $\pm$ SD of three separate experiments. Asterisk represents a $P < 0.01$ compared with cells co-transfected with empty pcDNA3.1 vector.

with an average increasing of 6.0-fold in THP-1 cells and 4.1-fold in Vero cells compared with that in cells co-transfected with pcDNA3.1 empty vector. There was no significant difference in relative luciferase activity
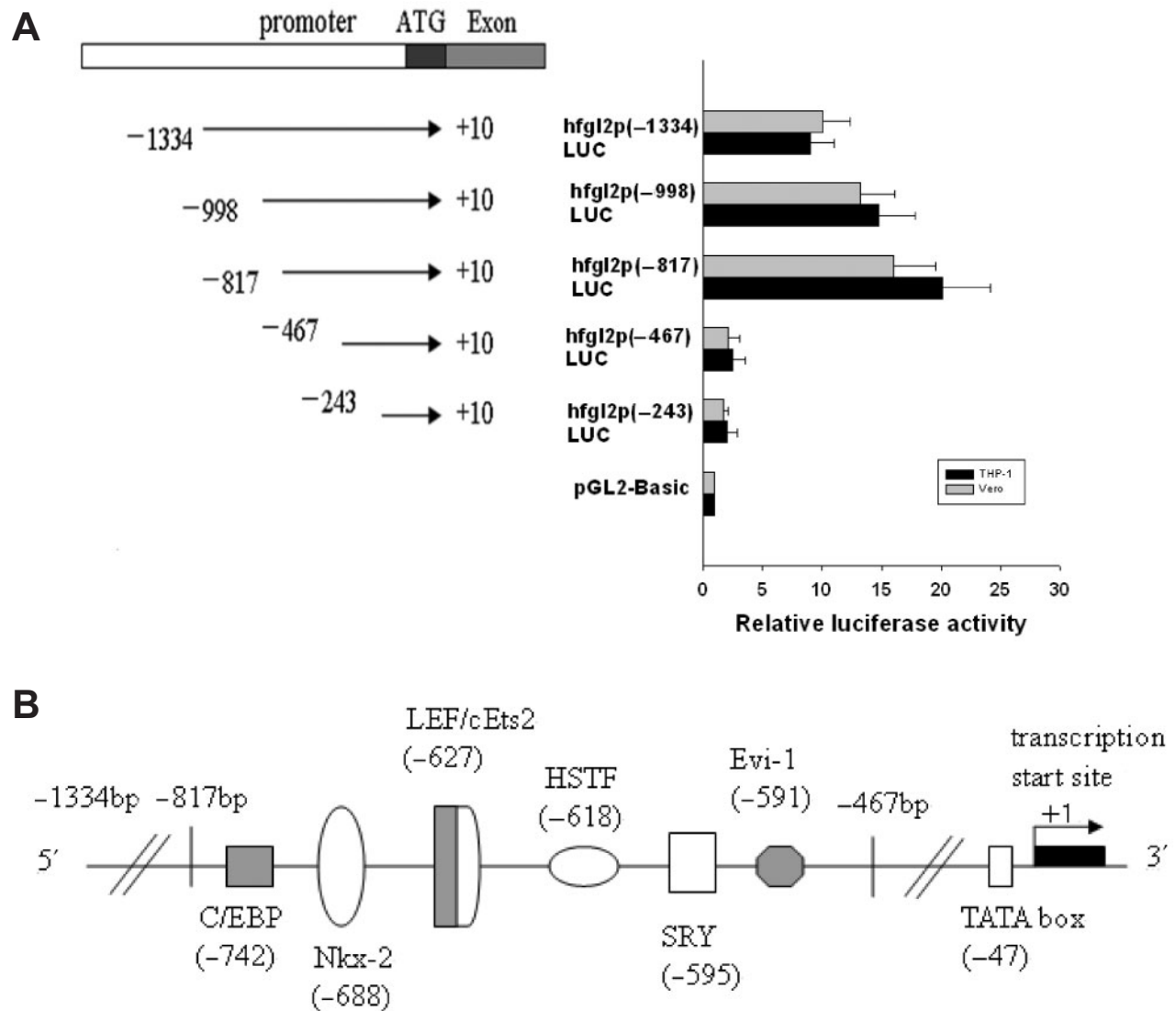
A

B

Fig. 7. **Corresponding hfgl2 promoter region in response to SARS-CoV N protein and its putative regulatory elements.** (A) Mapping of hfgl2 promoter in response to SARS-CoV N protein. The pcDNA-N plasmid was co-transfected with progressive deletions of hfgl2 promoter luciferase-reporter constructions into CHO cells, respectively. The cells transfected with pGL2-Basic vectors was control group. After transfection for 40–44 h, cells were harvested for measurement of relative luciferase activity. (B) Schematic representation of the putative regulatory elements in the putative (-817 to -467) hfgl2 promoter in response to N protein of SARS-CoV. Also shown are the transcription start site and the location of the TATA box.

when pcDNA-M or pcDNA-S2 was co-transfected with hfgl2p(-1334)LUC compared with pcDNA3.1 empty group in both cell lines. These results suggest that SARS-CoV N protein but not M or S2 protein induces hfgl2 promoter activity in CHO cells.

Mapping of the hfgl2 Promoter—To characterize the region in the hfgl2 promoter, which is responsive to N protein of SARS-CoV, constructs containing progressive deletion of the hfgl2 promoter were co-tranfected with pcDNA-N and a β-galactosidase vector in CHO cells. As shown in Fig. 7A, preliminary mapping of the hfgl2 promoter has defined a region from –817 to –467 to be responsive to induction of N protein of SARS-CoV. Using bioinformatics software (TESS and TFSEARCH), six putative *cis*-acting regulatory elements were identified within this region which included C/EBP (CCAAT enhancer binding protein), Nkx-2 (a tinman homoeodomain factor), HSTF (heat-shock transcription factor), SRY (a sex-determining region Y gene product), Evi-1 (an ectopic viral integration site 1 encoded factor) and an overlapped *cis*-element LEF-1 (lymphocyte enhancer factor-1)/c-Ets-2 (v-ets erythroblastosis virus E26 oncogene homologue 2) (Fig. 7B).

C/EBP Cis-Element Accounts for the Activation of hfgl2 Gene in Response to N protein of SARS-CoV—By site-directed mutagenesis, we were able to determine which of the six identified *cis*-elements were necessary for viral protein-induced transcription of hfgl2 gene. Six mutants within the hfgl2 promoter region were then constructed according to the manufacturer's protocol
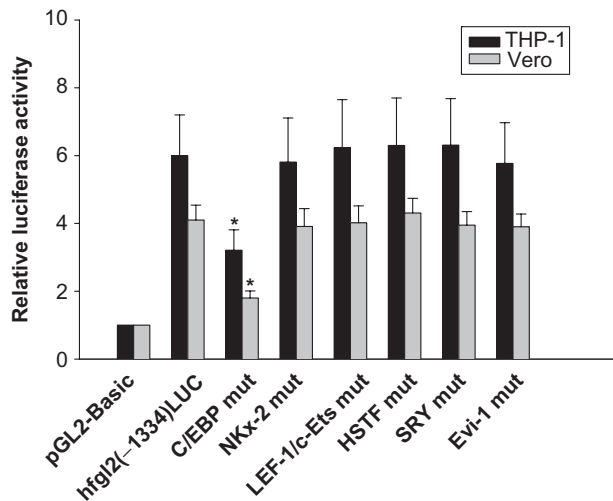
Fig. 8. **C/EBP *cis*-element accounts for the activation of hfgl2 gene in response to N protein of SARS-CoV.** Mutation assay showed transient expression of luciferase activity induced by the mutant variants in response to N protein of SARS-CoV in transfected THP-1 cells and Vero cells. pGL2-Basic vector was used as a negative control. Asterisk represents $P < 0.01$ compared with cells co-transfected with wild-type hfgl2p(-1334)LUC construct. All luciferase assays represent the mean ± SD of three separate experiments done in triplicate.

of QuickChange™ Site-directed Mutagenesis kit and confirmed correct by sequencing. Mutant hfgl2 promoter constructs were co-transfected with pcDNA-N in THP-1 cells and Vero cells followed by relative luciferase assay. In response to N protein, C/EBP mut resulted in a 46.5 and 56.1% decrease in THP-1 cells and in Vero cells in hfgl2 transcription activity relative to the wild-type hfgl2p(-1334)LUC construct whereas, Nkx-2mut, HSFmut, SRYmut and Evi-1mut had no statistical effect on transcription activity in response to N protein in the two cell lines (Fig. 8). Thus, these results suggested that C/EBP *cis*-element is necessary for the activation of the hfgl2 gene in response to N protein of SARS-CoV.

Transcription Factor C/EBP Alpha Binds to Its Cognate Cis-Element in the hfgl2 Promoter in Response to N Protein of SARS-CoV—By mutagenesis analysis we identified one candidate *cis*-elements for hfgl2 regulation in response to N protein of SARS-CoV. To further determine whether this *cis*-element binds nuclear extracts, EMSA assay was performed using ^{32}P-labelled C/EBP-hfgl2 probe and nuclear extracts from THP-1 cells and Vero cells transfected with pcDNA-N (Fig. 9). The results showed that there is one band when using the ^{32}P-labelled C/EBP-hfgl2 probe and the nuclear extracts from both THP-1 cells and Vero cells transfected with pcDNA-N. Furthermore, the binding of ^{32}P-labelled LEF/cEts-hfgl2 probe with the nuclear proteins in response to N protein could be shifted by adding antibody against CEBP alpha, but not by other non-specific antibody, suggesting that cellular transcription factor in nuclear extracts binds the C/EBP-hfgl2 *cis*-element.

DISCUSSION

From November 2002 when SARS broke out to July 2003 when the epidemic was interrupted, there were 8,098 cases globally with 774 deaths (available at: http://www.who.int/csr/sars/country/table2003_09_23/en/index.html. Accessed September 29, 2005). SARS-CoV has been confirmed as the pathogen of this new fatal infectious disease (*18*, *27*). Since then, much progress has been made in the virology and molecular characterization of SARS-CoV. Interests of researchers were focused on the replicase gene products which are important for viral replication, the structural proteins which are important for viral assembly and expression and functional studies of SARS-specific receptor, angiotensin converting enzyme 2 (ACE-2) (*28–31*). The interactions of SARS-CoV proteins and host genes were also recognized to be important in the pathogenesis of SARS.

In this paper, we constructed three eukaryotic expressing plasmids of SARS-CoV M, N and S2 protein. We examined and concluded that N protein could induce the expression of hfgl2 and thus activate the procoagulant activity of transfected cells. To define the mechanism of N protein inducing the hfgl2 gene, hfgl2 gene entire promoter was cloned and inserted into the pGL2-Basic vector, a promoter activity reporter. We found that N protein indeed activated the transcription of hfgl2 gene. Mapping of the hfgl2 gene promoter, the regulatory region was defined into the site of –817 to –467 (relative to transcription start site) in the hfgl2 promoter. The *cis*-elements responsible for the hfgl2 gene activation in response to N protein of SARS-CoV may be situated in this region theoretically. By Mutagenesis and EMSA assay, we further demonstrated that N protein induced activation of hfgl2 gene dependent on an important transcription factor C/EBP alpha, which has also been reported to be involved in the regulation of genes relevant to inflammation and carcinoma (*24*, *32*).

Our results confirmed that N protein of SARS-CoV activated hfgl2 expression both on the mRNA level and on the protein level. These findings were consistent with previous structural and functional analysis in response to N protein of SARS-CoV. The SARS-CoV N protein is a 46 kDa structural protein and was demonstrated to activate other host genes. N protein has also been reported to activate the activator protein 1 (AP1) signal transduction pathway and induce apoptosis in COS-1 cells in the absence of growth factors (*33*, *34*). SARS-CoV N protein can also significantly activate NF-κB only in Vero E6 cells, which are susceptible to SARS-CoV infection, but not in Vero or HeLa cells (*23*). Yan *et al.* (*24*) investigated the roles of SARS-CoV proteins in regulation of the pro-inflammatory factor, cyclooxygenase-2 (COX-2) and demonstrated that N protein could regulate COX-2 gene expression. EMSA and chromatin immunoprecipitation (CHIP) demonstrated that SARS-CoV N protein bound directly to a NF-kappaB-binding site and a CCAAT/enhancer binding protein (C/EBP)-binding site. Protein mutation analysis revealed that a Lys-rich motif of N protein acted as a nuclear localization signal and was essential for the activation of COX-2. Surjit *et al.* (*34*) showed that a short serine-rich stretch, a putative bipartite nuclear localization
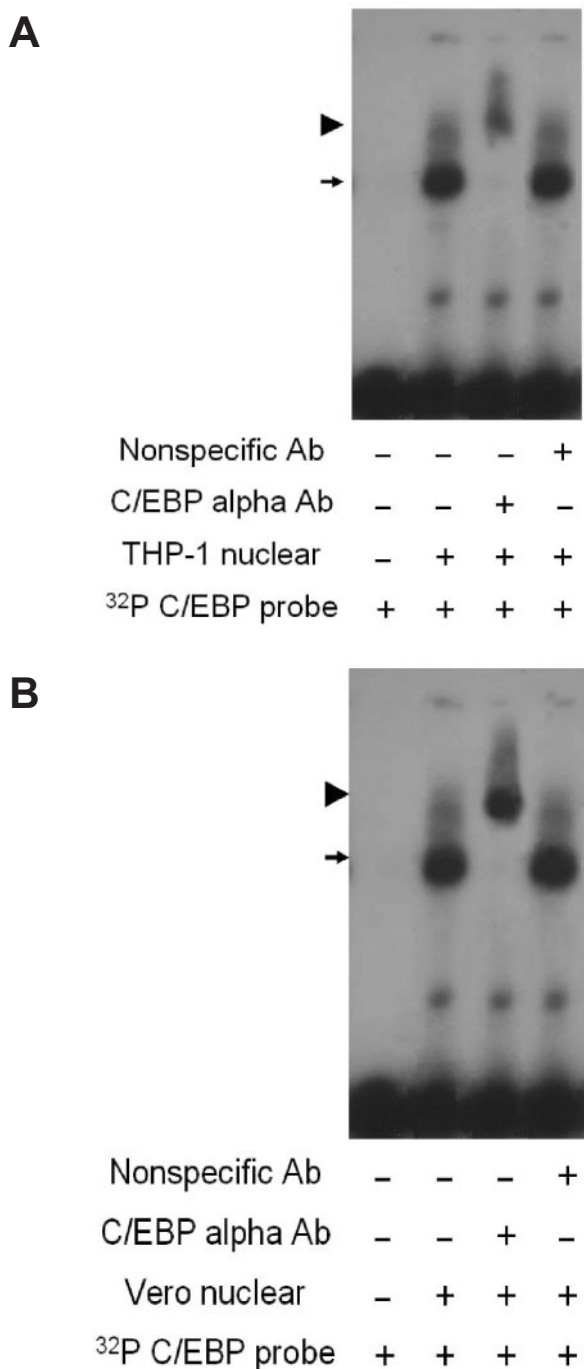
A

Nonspecific Ab   −   −   −   +
C/EBP alpha Ab   −   −   +   −
THP-1 nuclear   −   +   +   +
^{32}P C/EBP probe   +   +   +   +

B

Nonspecific Ab   −   −   −   +
C/EBP alpha Ab   −   −   +   −
Vero nuclear   −   +   +   +
^{32}P C/EBP probe   +   +   +   +

Fig. 9. **C/EBP alpha binds to its cognate *cis*-element in the hfgl2 promoter in response to N protein of SARS-CoV.** Nuclear extracts from THP-1 cells (A) and Vero cells (B) transfected with pcDNA-N were incubated with a ^{32}P-labelled probe, C/EBP-hfgl2, in the presence or absence of C/EBP alpha antibody. The binding of nuclear extract and its *cis*-element is denoted by an arrow, and the specific shift band by antibody against C/EBP alpha is indicated by an arrowhead.

signal and self association through a C-terminal 209 amino acid interaction domain characterize this protein. These studies elucidated the molecular mechanism of SARS-CoV N protein entering into nuclear and effecting

on host genes. However, Liao *et al*. (*23*) found that full-length N protein was located mainly in the cytoplasm and N1–225, N226–300 and N226–422 are located in both the cytoplasm and nucleus, and the latter two can also be found in the nucleus. The results from our experiments using the entire length of N gene are consistent with it. Our study showed that N protein expressed mainly in cytoplasm of cells transfected with pcDNA-N, which may be related with the distinct sequence and conformation of this SARS-CoV strain influencing its cellular localization. Chung *et al*. (*35*) reported that HBx protein-induced matrix metalloproteinase-9 gene activation was dependent on the transcription factor NF-κB and AP-1 and ERK and PI-3K/AKT signal pathway in the absence of HBx protein nucleoi localization. They suggest that stimulation of ERK and PI-3K/AKT signal pathways by HBx leads to the activation of NF-κB and AP-1 transcription factor. Then translocation of NF-κB and AP-1 activated by HBx into the nucleus results in an increase of MMP-9 expression. In our study, although the N protein expressed by constructed full-length of N sequence plasmid from patient's SARS-CoV isolate did not migrate to nucleus, but had the ability to induce hfgl2 expression. The truncated fragment of N protein may have the ability to enter to nucleus or the entire N protein or N fragments affect on a yet-not-identified signal molecule, and the nuclear localization of the signal molecule leads to hfgl2 up-regulated expression.

Fgl2 prothrombinase has been cloned and identified to belong to fibrinogen proteins family. It has been shown to have the attributes of a serine protease capable of directly cleaving prothrombin to thrombin leading to fibrin deposition. Previous work demonstrates mfgl2/hfgl2 expressed in liver plays a pivotal role in the pathogenesis of experimental and human hepatic failure (FHF) (*7–12*). Fgl2 prothrombinase gene could be regulated by cytokines, IFN-γ and TNF-α, and MHV-3 nucleocapsid protein with hepatic nuclear factor 4α as a key transcription factor (*9, 36, 37*). Activated fgl2 prothrombinase played its procoagulant role in the pathogenesis of fulminant hepatitis failure to contribute to the necrosis of hepatocytes (*11, 12*). Interestingly, both MHV-3 which induced the mfgl2 expression in Balb/cJ mouse and SARS-CoV which induced hfgl2 belong to coronavirus family.

Mapping of the promoter of hfgl2 gene determined the important regulatory region in the promoter from −817 to −467 (relative to transcription start site) and bioinformatics software provided some positive *cis*-acting regulatory transcription factors binding sites. We have found several putative *cis*-elements such as C/EBP, Nkx2, cEts-2 and HSF1 in the regulatory region. It was recently shown that the 7a protein of SARS-CoV induces biochemical changes associated with apoptosis. Data indicate that the induction of apoptosis by the 7a protein may be related to its ability to inhibit cellular translation and activate p38 MAPK (*38*). SARS-CoV 3a and 7a proteins induce apoptosis in mammalian cells was confirmed and membrane protein was currently identified to accelerated induction of apoptosis in insect cells (*39*). Although data showed that other proteins of SARS-CoV besides N protein were involved in gene expression

regulation and mechanism of apoptosis, our study showed that neither M nor S2 protein of SARS-CoV had effect on expression hfgl2 prothrombinase.

By mutagenesis and EMSA assay, we further found that N protein of SARS-CoV induced transcription of hfgl2 gene dependent on transcription factor C/EBP alpha. C/EBP form a subgroup within the basic region/leucine zipper superfamily of transcription factors (bZIP). Members of this family of transcription factors consist of an N-terminal transactivation domain, a DNA-binding basic region, and a leucine rich dimerization domain (*40*, *41*). There are six members of the C/EBP family (C/EBPα, C/EBPβ, C/EBPγ, C/EBPδ, C/EBPε and C/EBPζ). C/EBPα also named C/EBP alpha forms homodimers or heterodimers with other C/EBP proteins as well as with transcription factors of other families to precisely modulate the transcription of target genes (*42*). Phosphorylation and sumoylation of C/EBPα are suggested to be important regulatory mechanisms which cause changes in function of this protein (*43–45*). It was hypothesized that N protein of SARS-CoV activate transcription factor C/EBP alpha through phosphorylation or sumoylation, and then C/EBP forms homodimers that bind with its cognate *cis*-element in hfgl2 promoter to induce hfgl2 gene transcription.

Immuno-coagulation system took part in many serious diseases, such as myocardial infarction, sepsis, cancers, hepatic failure and so on. Fibrin or fibrinogen and its fragments in the pathophysiology coagulation derangements are part of these complex diseases. *Post-mortem* lung samples from six patients who died of SARS from April to July 2003 found fibrin deposition was universal phenomena besides formation of hyaline membranes, diffuse and bilateral lung consolidation and diffuse alveolar damage (*14*). It was concluded that diffuse damage of lung tissue in SARS patients was partly due to coagulation derangements. These derangements were implicated in the generation of microcirculation thrombosis, with deposition of microclots and obstruction of circulation, impairing blood flow and contributing to tissue hypoperfusion and consequently, organ dysfunction. As shown in SARS animal model, fgl2 prothrombinase gene and other cytokines, IFN-γ, TNF-α and chemoattractant protein 1 (MCP-1), participated in the development of SARS (*17*). In our study, the functional hfgl2 prothrombinase activity in a one-stage clotting assay was described and indicated that nucleocapsid protein could shorten clotting time markedly than other proteins. It suggested that nucleocapsid protein of SARS maybe the major agent resulting immuno-coagulation system. This study shed a slight light on the molecular mechanism of SARS and provided a molecular target of treatment in the future.

In conclusion, we demonstrated that the expression of hfgl2 prothrombinase was related with the N protein of SARS-CoV. Transcription factor C/EBP alpha plays an important role in inducing transcription of hfgl2 gene. This study illuminated that the SARS-CoV N protein may be involved in the pathogenesis of SARS and this finding can be used in the development of therapeutics of SARS.

REFERENCES

1. Halloran, P., Aprile, M., Haddad, G., and Robinette, M. (1982) The significance of elevated procoagulant activity in the monocytes of renal transplant recipients. *Transplant Proc.* **14**, 669–672
2. Tipping, P.G., Lowe, M.G., and Holdsworth, S.R. (1988) Glomerular macrophages express augmented procoagulant activity in experimental fibrin-related glomerulonephritis in rabbits. *J. Clin. Invest.* **82**, 1253–1259
3. Kucey, D.S., Cheung, P.Y., and Rotstein, O.D. (1992) Platelet-activating factor modulates endotoxin-induced macrophage procoagulant activity by a protein kinase C-dependent mechanism. *Infect. Immun.* **60**, 944–950
4. Levy, G.A., Leibowitz, J.L., and Edgington, T.S. (1981) Induction of monocyte procoagulant activity by murine hepatitis virus type 3 parallels disease susceptibility in mice. *J. Exp. Med.* **154**, 1150–1163
5. Parr, R.L., Fung, L., Reneker, J., Myers-Mason, N., Leibowitz, J.L., and Levy, G. (1995) Association of mouse fibrinogen-like protein with murine hepatitis virus-induced prothrombinase activity. *J. Virol.* **69**, 5033–5038
6. Qureshi, S.T., Clermont, S., Leibowitz, J., Fung, L.S., Levy, G., and Malo, D. (1995) Mouse hepatitis virus-3 induced prothrombinase (Fgl2) maps to proximal chromosome 5. *Genomics* **29**, 307–309
7. Levy, G.A., Liu, M., Ding, J., Yuwaraj, S., Leibowitz, J., Marsden, P.A., Ning, Q., Kovalinka, A., and Phillips, M.J. (2000) Molecular and functional analysis of the human prothrombinase gene (HFGL2) and its role in viral hepatitis. *Am. J. Pathol.* **156**, 1217–1225
8. Ding, J.W., Ning, Q., Liu, M.F., Lai, A., Peltekian, K., Fung, L., Holloway, C., Yeger, H., Phillips, M.J., and Levy, G.A. (1998) Expression of the fgl2 and its protein product (prothrombinase) in tissues during murine hepatitis virus strain-3 (MHV-3) infection. *Adv. Exp. Med. Biol.* **440**, 609–618
9. Ning, Q., Liu, M., Kongkham, P., Lai, M.M., Marsden, P.A., Tseng, J., Pereira, B., Belyavskyi, M., Leibowitz, J., Phillips, M.J., and Levy, G. (1999) The nucleocapsid protein of murine hepatitis virus type 3 induces transcription of the novel fgl2 prothrombinase gene. *J. Biol. Chem.* **274**, 9930–9936
10. Marazzi, S., Blum, S., Hartmann, R., Gundersen, D., Schreyer, M., Argraves, S., von Fliedner, V., Pytela, R., and Ruegg, C. (1998) Characterization of human fibroleukin, a fibrinogen-like protein secreted by T lymphocytes. *J. Immunol.* **161**, 138–147
11. Marsden, P.A., Ning, Q., Fung, L.S., Luo, X., Chen, Y., Mendicino, M., Ghanekar, A., Scott, J.A., Miller, T., Chan, C.W., Chan, M.W., He, W., Gorczynski, R.M., Grant, D.R., Clark, D.A., Phillips, M.J., and Levy, G.A. (2003) The Fgl2/fibroleukin prothrombinase contributes to immunologically mediated thrombosis in experimental and human viral hepatitis. *J. Clin. Invest.* **112**, 58–66
12. Zhu, C.L., Yan, W.M., Zhu, F., Zhu, Y.F., Xi, D., Tian, D.Y., Levy, G., Luo, X.P., and Ning, Q. (2005) Fibrinogen-like

protein 2 fibroleukin expression and its correlation with disease progression in murine hepatitis virus type 3-induced fulminant hepatitis and in patients with severe viral hepatitis B. *World J. Gastroenterol.* **11**, 6936–6940

13. Ning, Q., Sun, Y., Han, M., Zhang, L., Zhu, C., Zhang, W., Guo, H., Li, J., Yan, W., Gong, F., Chen, Z., He, W., Koscik, C., Smith, R., Gorczynski, R., Levy, G., and Luo, X. (2005) Role of fibrinogen-like protein 2 prothrombinase/ fibroleukin in experimental and human allograft rejection. *J. Immunol.* **174**, 7403–7411

14. Pei, F., Zheng, J., Gao, Z.F., Zhong, Y.F., Fang, W.G., Gong, E.C., Zou, W.Z., Wang, S.L., Gao, D.X., Xie, Z.G., Lu, M., Shi, X.Y., Liu, C.R., Yang, J.P., Wang, Y.P., Han, Z.H., Shi, X.H., Dao, W.B., and Gu, J. (2005) [Lung pathology and pathogenesis of severe acute respiratory syndrome: a report of six full autopsies]. *Zhonghua Bing Li Xue Za Zhi* **34**, 656–660

15. Hwang, D.M., Chamberlain, D.W., Poutanen, S.M., Low, D.E., Asa, S.L., and Butany, J. (2005) Pulmonary pathology of severe acute respiratory syndrome in Toronto. *Mod. Pathol.* **18**, 1–10

16. Robertson, M. (2003) Fgl2: link between hepatitis B and SARS? *Drug Discov. Today* **8**, 768–770

17. De Albuquerque, N., Baig, E., Ma, X., Zhang, J., He, W., Rowe, A., Habal, M., Liu, M., Shalev, I., Downey, G.P., Gorczynski, R., Butany, J., Leibowitz, J., Weiss, S.R., McGilvray, I.D., Phillips, M.J., Fish, E.N., and Levy, G.A. (2006) Murine hepatitis virus strain 1 produces a clinically relevant model of severe acute respiratory syndrome in A/J mice. *J. Virol.* **80**, 10382–10394

18. Drosten, C., Gunther, S., Preiser, W., van der Werf, S., Brodt, H.R., Becker, S., Rabenau, H., Panning, M., Kolesnikova, L., Fouchier, R.A., Berger, A., Burguiere, A.M., Cinatl, J., Eickmann, M., Escriou, N., Grywna, K., Kramme, S., Manuguerra, J.C., Muller, S., Rickerts, V., Sturmer, M., Vieth, S., Klenk, H.D., Osterhaus, A.D., Schmitz, H., and Doerr, H.W. (2003) Identification of a novel coronavirus in patients with severe acute respiratory syndrome. *N. Engl. J. Med.* **348**, 1967–1976

19. Marra, M.A., Jones, S.J., Astell, C.R., Holt, R.A., Brooks-Wilson, A., Butterfield, Y.S., Khattra, J., Asano, J.K., Barber, S.A., Chan, S.Y., Cloutier, A., Coughlin, S.M., Freeman, D., Girn, N., Griffith, O.L., Leach, S.R., Mayo, M., McDonald, H., Montgomery, S.B., Pandoh, P.K., Petrescu, A.S., Robertson, A.G., Schein, J.E., Siddiqui, A., Smailus, D.E., Stott, J.M., Yang, G.S., Plummer, F., Andonov, A., Artsob, H., Bastien, N., Bernard, K., Booth, T.F., Bowness, D., Czub, M., Drebot, M., Fernando, L., Flick, R., Garbutt, M., Gray, M., Grolla, A., Jones, S., Feldmann, H., Meyers, A., Kabani, A., Li, Y., Normand, S., Stroher, U., Tipples, G.A., Tyler, S., Vogrig, R., Ward, D., Watson, B., Brunham, R.C., Krajden, M., Petric, M., Skowronski, D.M., Upton, C., and Roper, R.L. (2003) The Genome sequence of the SARS-associated coronavirus. *Science* **300**, 1399–1404

20. Rota, P.A., Oberste, M.S., Monroe, S.S., Nix, W.A., Campagnoli, R., Icenogle, J.P., Penaranda, S., Bankamp, B., Maher, K., Chen, M.H., Tong, S., Tamin, A., Lowe, L., Frace, M., DeRisi, J.L., Chen, Q., Wang, D., Erdman, D.D., Peret, T.C., Burns, C., Ksiazek, T.G., Rollin, P.E., Sanchez, A., Liffick, S., Holloway, B., Limor, J., McCaustland, K., Olsen-Rasmussen, M., Fouchier, R., Gunther, S., Osterhaus, A.D., Drosten, C., Pallansch, M.A., Anderson, L.J., and Bellini, W.J. (2003) Characterization of a novel coronavirus associated with severe acute respiratory syndrome. *Science* **300**, 1394–1389

21. Kopecky-Bromberg, S.A., Martinez-Sobrido, L., and Palese, P. (2006) 7a protein of severe acute respiratory syndrome coronavirus inhibits cellular protein synthesis and activates p38 mitogen-activated protein kinase. *J. Virol.* **80**, 785–793

22. Law, A.H., Lee, D.C., Cheung, B.K., Yim, H.C., and Lau, A.S. (2007) A role for the non-structural Protein-1 of SARS-coronavirus in chemokine dysregulation. *J Virol.* **81**, 416–422

23. Liao, Q.J., Ye, L.B., Timani, K.A., Zeng, Y.C., She, Y.L., Ye, L., and Wu, Z.H. (2005) Activation of NF-kappaB by the full-length nucleocapsid protein of the SARS coronavirus. *Acta Biochim. Biophys. Sin.* **37**, 607–612

24. Yan, X., Hao, Q., Mu, Y., Timani, K.A., Ye, L., Zhu, Y., and Wu, J. (2006) Nucleocapsid protein of SARS-CoV activates the expression of cyclooxygenase-2 by binding directly to regulatory elements for nuclear factor-kappa B and CCAAT/enhancer binding protein. *Int. J. Biochem. Cell Biol.* **38**, 1417–1428

25. Chinese, S.M.E.C. (2004) Molecular evolution of the SARS coronavirus during the course of the SARS epidemic in China. *Science* **303**, 1666–1669

26. Ning, Q., Brown, D., Parodo, J., Cattral, M., Gorczynski, R., Cole, E., Fung, L., Ding, J.W., Liu, M.F., Rotstein, O., Phillips, M.J., and Levy, G. (1998) Ribavirin inhibits viral-induced macrophage production of TNF, IL-1, the procoagulant fgl2 prothrombinase and preserves Th1 cytokine production but inhibits Th2 cytokine response. *J. Immunol.* **160**, 3487–3493

27. Peiris, J.S., Lai, S.T., Poon, L.L., Guan, Y., Yam, L.Y., Lim, W., Nicholls, J., Yee, W.K., Yan, W., Cheung, M.T., Cheng, V.C., Chan, K.H., Tsang, D.N., Yung, R.W., Ng, T.K., and Yuen, K.Y. (2003) Coronavirus as a possible cause of severe acute respiratory syndrome. *Lancet* **361**, 1319–1325

28. Li, W., Moore, M.J., and Vasilieva, N. (2003) Angiotensin-converting enzyme 2 is a functional receptor for the SARS coronavirus. *Nature* **426**, 450–454

29. Turner, A.J., Hiscox, J.A., and Hooper, N.M. (2004) ACE2: from vasopeptidase to SARS virus receptor. *Trends Pharmacol. Sci.* **25**, 291–294

30. Towler, P., Staker, B., and Prsad, S.G. (2004) ACE2 X-ray structures reveal a large hinge-bending motion important for inhibitor binding and catalysis. *J. Biol. Chem.* **279**, 17996–18007

31. Prabakaran, P., Xiao, X., and Dimitrov, D.S. (2004) A model of the ACE2 structure and function as a SARS-CoV receptor. *Biochem. Biophys. Res. Commun.* **314**, 235–241

32. Paz-Priel, I., Cai, D.H., Wang, D., Kowalski, J., Blackford, A., Liu, H., Heckman, C.A., Gombart, A.F., Koeffler, H.P., Boxer, L.M., and Friedman, A.D. (2005) CCAAT/enhancer binding protein alpha (C/EBPalpha) and C/EBPalpha myeloid oncoproteins induce bcl-2 via interaction of their basic regions with nuclear factor-kappaB p50. *Mol. Cancer Res.* **3**, 585–596

33. He, R., Leeson, A., and Andonov, A. (2003) Activation of AP-1 signal transduction pathway by SARS coronavirus nucleocapsid protein. *Biochem. Biophys. Res. Commun.* **311**, 870–876

34. Surjit, M., Liu, B., and Jameel, S. (2004) The SARS coronavirus nucleocapsid protein induces actin reorganization and apoptosis in COS-1 cells in the absence of growth factors. *Biochem. J.* **383**, 13–18

35. Chung, T.W., Lee, Y.C., and Kim, C.H. (2004) Hepatitis B viral HBx induces matrix metalloproteinase-9 gene expression through activation of ERK and PI-3K/AKT pathways: involvement of invasive potential. *FASEB J.* **18**, 1123–1125

36. Liu, M., Mendicino, M., Ning, Q., Ghanekar, A., He, W., McGilvray, I., Shalev, I., Pivato, D., Clark, D.A., Phillips, M.J., and Levy, G.A. (2006) Cytokine-induced hepatic apoptosis is dependent on FGL2/fibroleukin: the role of Sp1/Sp3 and STAT1/PU.1 composite cis elements. *J. Immunol.* **176**, 7028–7038

37. Ning, Q., Lakatoo, S., Liu, M., Yang, W., Wang, Z., Phillips, M.J., and Levy, G.A. (2003) Induction of

prothrombinase fgl2 by the nucleocapsid protein of virulent mouse hepatitis virus is dependent on host hepatic nuclear factor-4 alpha. *J. Biol. Chem.* **278**, 15541–15549

38. Kopecky-Bromberg, S.A., Martinez-Sobrido, L., and Palese, P. (2006) 7a protein of severe acute respiratory syndrome coronavirus inhibits cellular protein synthesis and activates p38 mitogen-activated protein kinase. *J. Virol.* **80**, 785–793

39. Lai, C.W., Chan, Z.R., and Yang, D.G. (2006) Accelerated induction of apoptosis in insect cells by baculovirus-expressed SARS-CoV membrane protein. *FEBS Lett.* **580**, 3829–3834

40. Vinson, C.R., Sigler, P.B., and McKnight, S.L. (1989) Scissors-grip model for DNA recognition by a family of leucine zipper proteins. *Science* **246**, 911–916

41. Williams, S.C., Cantwell, C.A., and Johnson, P.F. (1991) A family of C/EBP-related proteins capable of forming covalently linked leucine zipper dimers in vitro. *Genes Dev.* **5**, 1553–1567

42. Lekstrom-Himes, J. and Xanthopoulos, K.G. (1998) Biological role of the CCAAT/enhancer-binding protein family of transcription factors. *J. Biol. Chem.* **273**, 28545–28548

43. Liu, H.K., Perrier, S., Lipina, C., Finlay, D., McLauchlan, H., Hastie, C.J., Hundal, H.S., and Sutherland, C. (2006) Functional characterisation of the regulation of CAAT enhancer binding protein alpha by GSK-3 phosphorylation of Threonines 222/226. *BMC Mol. Biol.* **7**, 14

44. Geletu, M., Balkhi, M.Y., Peer Zada, A.A., Christopeit, M., Pulikkan, J.A., Trivedi, A.K., Tenen, D.G., and Behre, G. (2007) Target proteins of C/EBPalphap30 in AML: C/EBPalphap30 enhances sumoylation of C/EBPalphap42 via up-regulation of Ubc9. *Blood* **110**, 3301–3309

45. Sato, Y., Miyake, K., Kaneoka, H., and Iijima, S. (2006) Sumoylation of CCAAT/enhancer-binding protein alpha and its functional roles in hepatocyte differentiation. *J. Biol. Chem.* **281**, 21629–21639